Absorption with inversion and amplification without inversion in a coherently prepared V system: A dressed-state approach

D. Braunstein and R. Shuker*
Department of Physics, Ben Gurion University of the Negev, 84105 Beer Sheva, Israel
(Received 14 March 2001; published 12 October 2001)

Light-induced absorption with population inversion and amplification without population inversion in a coherently prepared closed three level V-type system are investigated. This study is performed from the point of view of a two color dressed-state basis. Both of these processes are possible due to atomic coherence and quantum interference contrary to simple intuitive predictions. Merely on a physical basis, one would expect a complementary process to the amplification without inversion. We believe that absorption in the presence of population inversion found in the dressed-state picture utilized in this study, constitutes such a process. We derive approximate analytic time-dependent solutions, for coherences and populations that are compared with full numerical solutions exhibiting good agreement. Steady-state quantities are also calculated, and the conditions under which the system exhibits absorption and gain with and without inversion, in the dressed-state representation are derived. It is found that for weak input probe-laser field absorption with inversion and amplification without inversion may occur, for a range of system parameters. These take place at resonance and the generalized Rabi ac Stark-shifted frequencies, in agreement with exprimental investigations, and at beat frequencies, depending on the relevant parameters.

DOI: 10.1103/PhysRevA.64.053812 PACS number(s): 42.50.Ct, 42.50.Gy

I. INTRODUCTION

Recently there has been tremendous interest in the study of light amplification and lasing without the requirement of population inversion (LWI), potentially capable of extending the range of laser devices to a spectral region in which, for various reasons, population inversion is difficult to achieve. These spectral regions include UV that can be obtained from atomic vapor, and mid-to-far infrared, obtained by intersubband transitions in quantum wells. Many models for LWI have been proposed, mostly three and four level schemes, in Λ and V configurations. The dependence of optical gain on system parameters has also been investigated [1–19].

The key mechanism, which is common to most of the proposed schemes, is the utilization of external coherent fields, which induce quantum coherence and interference in multilevel systems. An exception of LWI without the use of coherent fields was also reported [9]. In particular, it was shown that if atomic coherence between certain atomic states is established, different absorption processes may interfere destructively, leading to the reduction or even the cancellation of absorption [7,13]. At the same time, stimulated emission may remain intact, leading to the possibility of gain even if only a small fraction of the population is in the excited state.

Experimental observations of inversionless gain and lasing without inversion have been reported by several groups [20–25]. Off-resonance [20] and on-resonance [21,22] gain were reported.

Inversionless lasers have been shown to have unique properties such as nonclassical photon statistics and substantially narrow spectral features [26,27]. In a recent paper, Y. Zhu [12] analyzed the transient and steady-state properties of light amplification without population inversion in a closed, three-level V-type system in the bare-state basis. Steady-state dressed-state populations were also calculated, in the limit of a strong driving laser.

In this paper we study a V-type three-level model within the framework of the dressed-state basis, and give explicit analytic time-dependent solutions, as well as steady-state solutions for populations and coherences for the case of a strong drive field. This paper details the calculations of LWI in the dressed-state basis, which is valid to atoms dressed both by the pump and probe lasers. Moreover, we offer a set of theoretical tools allowing one to obtain explicit time-dependent solutions for populations and coherences. These calculations show the possibility of inversion and inversionless gain in the dressed basis, as well as gain without population inversion in the bare-state representation. Our study shows explicitly the existence of absorption despite population inversion (ADI). Although this effect is contrary to a simple physical intuitive explanation of absorption, this process has a conceptual reasoning. From basic physical arguments, one expects a complementary process to amplification without inversion. We believe that absorption in the presence of population inversion, found in the dressed-state picture, constitutes such a process [18]. It is another manifestation of the quantum interference that may occur in multilevel systems where coherently prepared states present the possibility of interfering channels [28]. This phenomenon should be interpreted as a quantum interference constructive process for the stimulated absorption, just as LWI is obtained from a quantum interference *destructive* process of absorption. Such a phenomenon was alluded to in the work of Marlan O. Scully and Shi-Yao Zhu [18].

In Sec. II, we present the model system and the master equation used to derive the equations of motion for the elements of the density matrix. We have chosen to employ a fully quantum-mechanical Hamiltonian, even though later on, the density-matrix equations are reduced to their semi-

*Email address: shuker@bgumail.bgu.ac.il

classical version. The quantum-mechanical Hamiltonian gives rise to a simple picture of the stationary dressed-states. In Sec. III, the dressed levels are introduced and the master equation is projected over the dressed-state basis. Physical interpretation of relaxation coefficients in the dressed basis is given and the role that quantum coherences and interferences play is elucidated. In Sec. IV, we present approximate time-dependent and steady-state analytic solutions for the dressed-state populations and coherences. Comparison is made with the bare-state results. In Sec. V, a short sketch of a calculation of the active frequencies is presented. It is performaed by a unitary transformation of the time-dependent density matrix from the interaction picture into the Schrödinger one. The resulting time-dependent elements of the density matrix are then Fourier transformed into the frequaency domain in order to extract the relevant frequencies at which LWI and ADI may take place for an appropriate set of parameters. Section VI summarizes the findings of our calculations and draws conclusions.

II. HAMILTONIAN AND MASTER EQUATION FOR THE ATOM

Let us consider the closed *V*-type three level system illustrated in Fig. 1. The transition $|a\rangle \leftrightarrow |b\rangle$ of frequency ω_{ba} is driven by a strong, single-mode laser of frequency ω_L. The transition $|a\rangle \leftrightarrow |c\rangle$ of frequency ω_{ca} is pumped incoherently with a rate Λ. A single-mode probe laser (not necessarily weak) is applied to the transition $|a\rangle \leftrightarrow |c\rangle$. γ_b (γ_c) is the spontaneous emission rate from the state $|b\rangle$ ($|c\rangle$). The states $|b\rangle$ and $|c\rangle$ are not directly coupled.

We have chosen to work within the frame of the master equation for the atom, since it being an operator equation independent of representation, it can be projected over any basis. We use a generalization of a standard master equation adjusted to account for the scheme described above [29]. The master equation is given by

$$\begin{aligned}\dot{\sigma} = & -\frac{i}{\hbar}[H,\sigma] - \frac{\gamma_b}{2}[s_+ s_- \sigma + \sigma s_+ s_-] + \gamma_b s_- \sigma s_+ \\ & - \frac{\gamma_c}{2}[s'_+ s'_- \sigma + \sigma s'_+ s'_-] + \gamma_c s'_- \sigma s'_+ \\ & - \frac{\Lambda}{2}[s'_+ s'_- \sigma + \sigma s'_+ s'_-] - \frac{\Lambda}{2}[s'_- s'_+ \sigma + \sigma s'_- s'_+] \\ & + \Lambda s'_+ \sigma s'_- + \Lambda s'_- \sigma s'_+ . \end{aligned} \tag{1}$$

Here, σ is the density operator for the atom, $s_+(s_-)$, $s'_+(s'_-)$ are the atomic raising and lowering operators, for the $|a\rangle \leftrightarrow |b\rangle$ and $|a\rangle \leftrightarrow |c\rangle$ transitions, respectively. H is the Hamiltonian of the global system and we take it to be fully quantum mechanical. The quantum-mechanical Hamiltonian gives rise to a simple picture of the stationary dressed-states. The Hamiltonian in the dipole and rotating wave approximation is given by

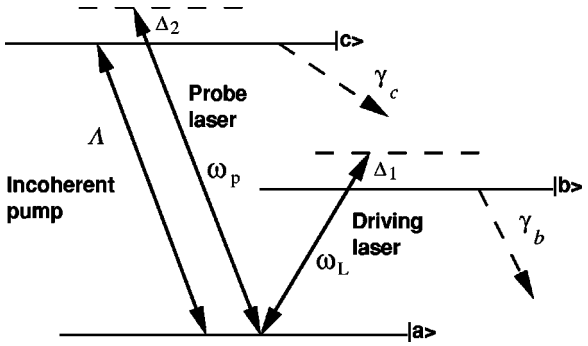

FIG. 1. A three level V-type system for LWI.

$$\begin{aligned} H = & \hbar\omega_{ba}|b\rangle\langle b| + \hbar\omega_{ca}|c\rangle\langle c| + \hbar\omega_L\left(a^\dagger a + \frac{1}{2}\right) \\ & + \hbar\omega_p\left(a'^\dagger a' + \frac{1}{2}\right) + g(s_+ a + s_- a^\dagger) \\ & + g'(s'_+ a' + s'_- a'^\dagger). \end{aligned} \tag{2}$$

g and g' are coupling constants and are assumed to be real. The eigenstates of the unperturbed part of the Hamiltonian form a three-dimensional manifold labeled by the atomic indexes, the laser photon number N and by the probe photon number N'. The manifold is written

$$\varepsilon(N,N') = \{|a,N+1,N'+1\rangle, |b,N,N'+1\rangle, |c,N+1,N'\rangle\}. \tag{3}$$

We represent the uncoupled eigenstates of the atom and the two noninteracting field modes as

$$|a,N+1,N'+1\rangle = \begin{pmatrix} 1 \\ 0 \\ 0 \end{pmatrix}, \quad |b,N,N'+1\rangle = \begin{pmatrix} 0 \\ 1 \\ 0 \end{pmatrix},$$

$$|c,N+1,N'\rangle = \begin{pmatrix} 0 \\ 0 \\ 1 \end{pmatrix}. \tag{4}$$

In this basis, the Hamiltonian takes the form

$$H_{Int} = \begin{pmatrix} 0 & -\Omega & -G \\ -\Omega & -\Delta_1 & 0 \\ -G & 0 & -\Delta_2 \end{pmatrix}, \tag{5}$$

where we have defined the Rabi frequencies and the detunings, in their quantum form by

$$-g\sqrt{N+1} = \hbar\Omega; \quad -g'\sqrt{N'+1} = \hbar G;$$

$$\Delta_1 = \omega_L - \omega_{ba}; \quad \Delta_2 = \omega_p - \omega_{ca}. \tag{6}$$

To obtain the semiclassical equations of motion for the elements of the density matrix we project the master equa-

tion (1) over the basis (4) and perform the following reduction operation by introducing the reduced populations and coherences ρ_{ij} via

$$\rho_{aa}=\sum_{N,N'}\langle a,N+1,N'+1|\sigma|a,N+1,N'+1\rangle, \quad (7a)$$

$$\rho_{ab}=\sum_{N,N'}\langle a,N+1,N'+1|\sigma|b,N,N'+1\rangle, \quad (7b)$$

and similar relations for the other populations and coherences. Taking into account the above-reduced quantities, we obtain the density-matrix equations [19]

$$\dot{\rho}_{aa}=-\Lambda\rho_{aa}+(\Lambda+\gamma_c)\rho_{cc}+\gamma_b\rho_{bb}+i\Omega(\rho_{ba}-\rho_{ab})+iG(\rho_{ca}-\rho_{ac}), \quad (8a)$$

$$\dot{\rho}_{bb}=-\gamma_b\rho_{bb}+i\Omega(\rho_{ab}-\rho_{ba}), \quad (8b)$$

$$\dot{\rho}_{cc}=\Lambda\rho_{aa}-(\Lambda+\gamma_c)\rho_{cc}+iG(\rho_{ac}-\rho_{ca}), \quad (8c)$$

$$\dot{\rho}_{ab}=-\left[\frac{1}{2}(\Lambda+\gamma_b)+i\Delta_1\right]\rho_{ab}+i\Omega(\rho_{bb}-\rho_{aa})+iG\rho_{cb}, \quad (8d)$$

$$\dot{\rho}_{ac}=-\left[\frac{1}{2}(\Lambda+\gamma_c)+i\Delta_2\right]\rho_{ac}+iG(\rho_{cc}-\rho_{aa})+i\Omega\rho_{bc}, \quad (8e)$$

$$\dot{\rho}_{bc}=-\left[\frac{1}{2}(\Lambda+\gamma_b+\gamma_c)+i(\Delta_2-\Delta_1)\right]\rho_{bc}+i\Omega\rho_{ac}-iG\rho_{ba}. \quad (8f)$$

III. DRESSED STATES AND DENSITY-MATRIX EQUATIONS IN THE DRESSED-STATE BASIS

The dressed states are obtained by finding the eigenvectors of the interaction Hamiltonian, Eq. (5). To simplify things a little, we take both the driving laser field and the probe field to be in exact resonance with the corresponding bare state transitions, i.e., we take $\Delta_1=\Delta_2=0$. When the detunings are set to zero, we notice that the energies in the bare-state basis are all degenerate, and in fact, equal to zero (in the interaction picture). Carrying out the diagonalization procedure, we obtain the following eigenstates:

$$|\alpha(N)(N')\rangle=-\frac{G}{R}|b,N,N'+1\rangle+\frac{\Omega}{R}|c,N+1,N'\rangle, \quad (9a)$$

$$|\beta(N)(N')\rangle=-\frac{1}{\sqrt{2}}|a,N+1,N'+1\rangle+\frac{\Omega}{\sqrt{2}R}|b,N,N'+1\rangle+\frac{G}{\sqrt{2}R}|c,N+1,N'\rangle, \quad (9b)$$

$$|\gamma(N)(N')\rangle=\frac{1}{\sqrt{2}}|a,N+1,N'+1\rangle+\frac{\Omega}{\sqrt{2}R}|b,N,N'+1\rangle+\frac{G}{\sqrt{2}R}|c,N+1,N'\rangle, \quad (9c)$$

and the corresponding energies

$$E_{|\gamma\rangle}=-\hbar R;\quad E_{|\alpha\rangle}=0;\quad E_{|\beta\rangle}=\hbar R, \quad (10)$$

where we have introduced the on resonance, two field generalized Rabi flopping frequency $R=\sqrt{\Omega^2+G^2}$.

Note that for the case $G=0$, Eqs. (9b) and (9c) render the usual coupling and non-coupling dressed-states, while the $|\alpha\rangle$ state, which is identical to the $|c\rangle$ state, is not involved in the interaction altogether. The energy ladder is shown schematically in Fig. 2. We can see that one state remained intact, while the other two states were displaced by an energy amount of $\hbar R$, with respect to the bare states. In the strong driving field limit, i.e., when $\Omega\gg G$, we see that the $|\alpha(N)(N')\rangle$ state has the character of the excited bare state $|c,N+1,N'\rangle$, and hence, is expected to be less populated than the other two states. By contrast, the $|\beta(N)(N')\rangle$ and $|\gamma(N)(N')\rangle$ states have a ground-state character, and hence, will be more populated than the $|\alpha(N)(N')\rangle$ state. However, both $|\beta\rangle$ and $|\gamma\rangle$ states are also contaminated by the same amount of the first excited level, and thus, they are expected to possess the same population content.

The eigenstates of Eqs. (9a)–(9c) define a rotation matrix (transformation matrix)

$$T=\begin{pmatrix} 0 & -\frac{G}{R} & \frac{\Omega}{R} \\ -\frac{1}{\sqrt{2}} & \frac{\Omega}{\sqrt{2}R} & \frac{G}{\sqrt{2}R} \\ \frac{1}{\sqrt{2}} & \frac{\Omega}{\sqrt{2}R} & \frac{G}{\sqrt{2}R} \end{pmatrix} \quad (11)$$

that diagonalizes the Hamiltonian of Eq. (5) via the matrix product THT^{-1}. Thus, the density operator in the dressed atom basis, ρ^D, will be given by the matrix product

$$\rho^D=T\rho^B T^{-1}, \quad (12)$$

where ρ^B is the density operator in the bare basis.

Projection of the master equation over the dressed-state basis yields particularly simple equations for the first part of Eq. (1), i.e., the Hamiltonian part of the master equation. However, in the dressed atom basis, the relaxation terms of Eq. (1) give rise to equations that are not as simple as Eqs. (8a)–(8f). In particular, couplings between dressed-state populations and coherences between two dressed-states appear. In the next section, we present an approximate version of the complete set of equations given bellow.

The equation of motion for the density-matrix elements in the dressed-state representation are given by

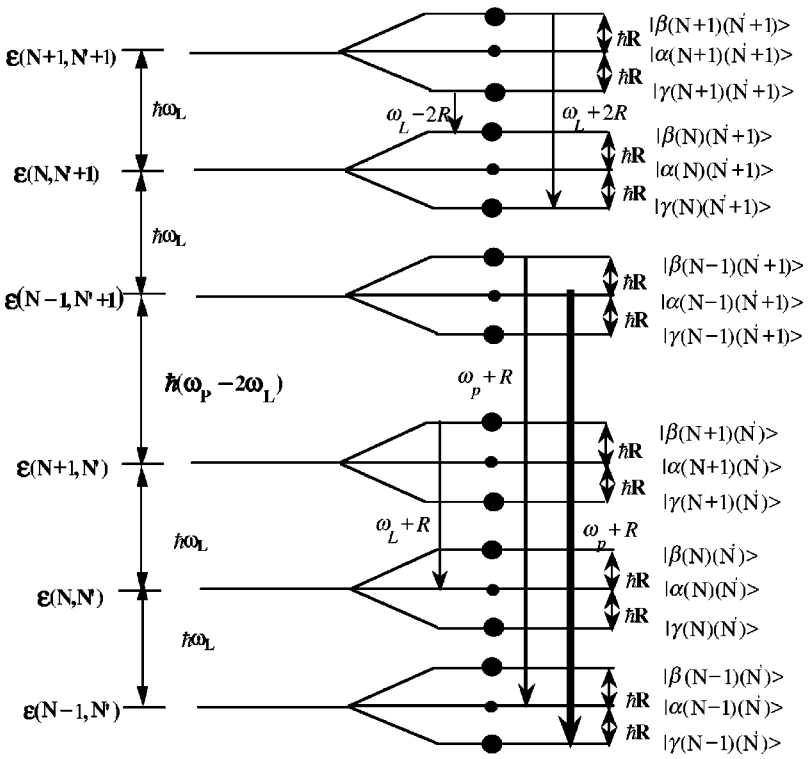

FIG. 2. Manifolds $\epsilon(N,N')$, $\epsilon(N+1,N')$, $\epsilon(N,N'+1)$, and $\epsilon(N+1,N'+1)$, etc., of uncoupled states of the atom + lasers photons (left-hand part). The dressed level (perturbed levels) are shown at the right-hand side. The circles represent steady-state populations.

$$\dot{\rho}_{\alpha\alpha}=-(\Gamma_\alpha+\Lambda')\rho_{\alpha\alpha}+\tilde{\Gamma}(\rho_{\alpha\beta}+\rho_{\beta\alpha})+\tilde{\Gamma}(\rho_{\alpha\gamma}+\rho_{\gamma\alpha})+\frac{1}{2}\Lambda'\rho_{\beta\beta}-\frac{1}{2}\Lambda'(\rho_{\beta\gamma}+\rho_{\gamma\beta})+\frac{1}{2}\Lambda'\rho_{\gamma\gamma}, \quad (13a)$$

$$\dot{\rho}_{\alpha\beta}=-(\Gamma_{\alpha\beta}-iR)\rho_{\alpha\beta}-\left(\Gamma_\beta-\frac{1}{4}\Lambda'\right)\rho_{\alpha\gamma}-\tilde{\Gamma}'\rho_{\beta\gamma}+(\tilde{\Gamma}-\tilde{\Gamma}')\rho_{\gamma\beta}+\tilde{\Gamma}\rho_{\alpha\alpha}+(\tilde{\Gamma}+\tilde{\Gamma}')\rho_{\beta\beta}+\tilde{\Gamma}'\rho_{\gamma\gamma}, \quad (13b)$$

$$\dot{\rho}_{\alpha\gamma}=-(\Gamma_{\alpha\beta}+iR)\rho_{\alpha\gamma}-\left(\Gamma_\beta-\frac{1}{4}\Lambda'\right)\rho_{\alpha\beta}+(\tilde{\Gamma}-\tilde{\Gamma}')\rho_{\beta\gamma}-\tilde{\Gamma}'\rho_{\gamma\beta}+\tilde{\Gamma}\rho_{\alpha\alpha}+\tilde{\Gamma}'\rho_{\beta\beta}+(\tilde{\Gamma}+\tilde{\Gamma}')\rho_{\gamma\gamma}, \quad (13c)$$

$$\dot{\rho}_{\beta\beta}=-\left(\Gamma_\beta+\frac{1}{2}\Lambda\right)\rho_{\beta\beta}+\frac{1}{2}(\Gamma_\alpha+\Lambda')\rho_{\alpha\alpha}+\left(\Gamma_\beta+\frac{1}{2}\Lambda-\frac{1}{2}\Lambda'\right)\rho_{\gamma\gamma}-\tilde{\Gamma}(\rho_{\alpha\gamma}+\rho_{\gamma\alpha})+\frac{1}{4}\Lambda'(\rho_{\beta\gamma}+\rho_{\gamma\beta}), \quad (13d)$$

$$\dot{\rho}_{\beta\gamma}=-(\Gamma_{\beta\gamma}+2iR)\rho_{\beta\gamma}-\left(\Gamma_\beta+\frac{1}{2}\Lambda-\frac{1}{2}\Lambda'\right)\rho_{\gamma\beta}+\tilde{\Gamma}(\rho_{\alpha\beta}+\rho_{\gamma\alpha})+2\tilde{\Gamma}(\rho_{\beta\alpha}+\rho_{\alpha\gamma})-\frac{1}{2}(\Gamma_\alpha+\Lambda')\rho_{\alpha\alpha}-\left(2\Gamma_\beta-\frac{1}{4}\Lambda'\right)(\rho_{\beta\beta}+\rho_{\gamma\gamma}), \quad (13e)$$

$$\dot{\rho}_{\gamma\gamma}=-\left(\Gamma_\beta+\frac{1}{2}\Lambda\right)\rho_{\gamma\gamma}-\tilde{\Gamma}(\rho_{\alpha\beta}+\rho_{\beta\alpha})+\frac{1}{4}\Lambda'(\rho_{\beta\gamma}+\rho_{\gamma\beta})+\frac{1}{2}(\Gamma_\alpha+\Lambda')\rho_{\alpha\alpha}+\left(\Gamma_\beta+\frac{1}{2}\Lambda-\frac{1}{2}\Lambda'\right)\rho_{\beta\beta}, \quad (13f)$$

where we have again made use of the reduction operation

$$\rho_{i,j}=\sum_{N,N'}\langle i(N)(N')|\sigma|j(N)(N')\rangle, \quad i,j=|\alpha\rangle,|\beta\rangle,|\gamma\rangle. \quad (14)$$

In obtaining Eqs. (13a)–(13f), we have introduced the following notation for the dressed picture decaying rates and relaxation coefficients

$$\Gamma_\alpha=\frac{1}{R^2}(\gamma_b G^2+\gamma_c\Omega^2), \quad \Gamma_\beta=\frac{1}{4R^2}(\gamma_b\Omega^2+\gamma_c G^2),$$

$$\Gamma_{\alpha\beta}=\Gamma_\beta+\frac{1}{2}(\Gamma_\alpha+\Lambda+\Lambda'/2), \quad \Gamma_{\beta\gamma}=3\Gamma_\beta+\frac{3}{2}\Lambda-\Lambda',$$

$$\tilde{\Gamma}=\frac{G\Omega}{2\sqrt{2}R^2}(\gamma_b-\gamma_c-\Lambda), \quad \tilde{\Gamma}'=\frac{G\Omega\Lambda}{2\sqrt{2}R^2}, \quad \Lambda'=\frac{\Lambda\Omega^2}{R^2}. \quad (15)$$

Γ_α, $\Gamma_\beta=\Gamma_\gamma$ are the spontaneous emission decay rate of the $|\alpha\rangle$, $|\beta\rangle$, and $|\gamma\rangle$ states. More precisely, the state $|\alpha(N)(N')\rangle$ decays by spontaneous emission with a rate Γ_α to the levels $|\beta(N-1)(N')\rangle$, $|\gamma(N-1)(N')\rangle$, $|\beta(N)(N'-1)\rangle$, and $|\gamma(N)(N'-1)\rangle$. Similarly, the levels $|\beta(N)(N')\rangle$, $|\gamma(N)(N')\rangle$ decay with the same rate Γ_β to the

same levels as $|\alpha(N)(N')\rangle$. The coherences $\rho_{\alpha\beta}$, and $\rho_{\alpha\gamma}$ ($\rho_{\beta\gamma}$) decay with a rate $\Gamma_{\alpha\beta}$ ($\Gamma_{\beta\gamma}$). Λ' is a dressed picture pump rate that causes population and depopulation of the dressed levels. It also has an important influence on the coherences as can readily be seen from Eqs. (13a)–(13f).

$\tilde{\Gamma}$ and $\tilde{\Gamma}'$ are identified as *interference terms*. They involve the product of two Rabi frequencies. Both parameters vanish whenever either G or Ω are zero. These terms are responsible for the amplification without inversion and for the absorption despite the inversion. This fact is verified numerically. When we have set both $\tilde{\Gamma}$ and $\tilde{\Gamma}'$ to zero (this happens when $\Lambda=0$ and $\gamma_b=\gamma_c$) any previously obtained gain has vanished. The first and second terms in $\Gamma_{\alpha\beta}$, Γ_β, and $\Gamma_\alpha/2$, describe damping of the atomic coherence due to radiative transitions of the levels involved to lower levels, and is equal to half the sum of all transition rates starting from $|\alpha(N)(N')\rangle$ and $|\beta(N)(N')\rangle$. The remaining terms in $\Gamma_{\alpha\beta}$ describe damping of the coherence $\rho_{\alpha\beta}$ due to the incoherent pump. The interpretation of $\Gamma_{\beta\gamma}$ is similar except that the $3\Gamma_\beta$ is composed of a $2\Gamma_\beta$ term responsible for the coherence damping due to radiative transition, plus a single Γ_β component resulting from the transfer of coherence from higher levels belonging to higher manifolds [29]. This fact would have been more transparent had we written the nonreduced version of Eqs. (13a)–(13f). Inspection of Eqs. (13) reveals that $\rho_{\alpha\beta}$ and $\rho_{\alpha\gamma}$ have the same free evolution frequency R, however they oscillate out of phase. The free evolution frequency of $\rho_{\beta\gamma}$ is twice as large, as both levels $|\beta\rangle$ and $|\gamma\rangle$ are contaminated by the bare ground-state $|a\rangle$. Note that the closure of the system is satisfied by Eqs. (13a)–(13f), i.e., $d/dt(\rho_{\alpha\alpha}+\rho_{\beta\beta}+\rho_{\gamma\gamma})=0$. Gain or absorption coefficient for the $|j\rangle\rightarrow|i\rangle$ transition is proportional to $\mathrm{Im}[\rho_{ij}]$. In our notation, amplification will occur if $\mathrm{Im}[\rho_{ij}]\rangle 0$.

In the next section, we present approximate solutions of Eqs. (13a)–(13f), both for the time-dependent and the steady-state solutions. These will be compared with numerical calculations of the full system, i.e., without any approximation.

IV. DENSITY-MATRIX EQUATIONS IN THE DRESSED-STATE BASIS IN THE SECULAR APPROXIMATION

As mentioned before, the Hamiltonian part of the master equation has a simple form in the dressed-state basis given by Eqs. (9a)–(9c) (the Hamiltonian is diagonalized in the dressed-state representation). The problem arises when the spontaneous emission and pump terms are present in the master equation, Eq. (1), giving the complicated couplings appearing in Eqs. (13a)–(13f). Solving exactly the complete set seems to be a formidable task even with the help of MATHEMATICA software [30]. However, the situation can be simplified if the frequency difference between the dressed states of the manifold, namely, the Rabi flopping frequency R is large compared with the rates G, γ_b, γ_c, and Λ, i.e., strong drive. We can then ignore the ''nonsecular'' terms, i.e., couplings between populations and coherences (see [29]).

A. The evolution of the population terms

When the ''nonsecular'' couplings between populations and coherences are ignored, we obtain from Eqs. (13a), (13d), and (13f) the following equations for the populations:

$$\dot{\rho}_{\alpha\alpha}=-(\Gamma_\alpha+\Lambda')\rho_{\alpha\alpha}+\frac{1}{2}\Lambda'\rho_{\beta\beta}+\frac{1}{2}\Lambda'\rho_{\gamma\gamma}, \quad (16a)$$

$$\dot{\rho}_{\beta\beta}=-\left(\Gamma_\beta+\frac{1}{2}\Lambda\right)\rho_{\beta\beta}+\frac{1}{2}(\Gamma_\alpha+\Lambda')\rho_{\alpha\alpha}+\left(\Gamma_\beta+\frac{1}{2}\Lambda-\frac{1}{2}\Lambda'\right)\rho_{\gamma\gamma}, \quad (16b)$$

$$\dot{\rho}_{\gamma\gamma}=-\left(\Gamma_\beta+\frac{1}{2}\Lambda\right)\rho_{\gamma\gamma}+\frac{1}{2}(\Gamma_\alpha+\Lambda')\rho_{\alpha\alpha}+\left(\Gamma_\beta+\frac{1}{2}\Lambda-\frac{1}{2}\Lambda'\right)\rho_{\beta\beta}. \quad (16c)$$

Note that population conservation is still maintained. The interpretation of Eqs. (16a)–(16c) is very clear. The state $|\alpha\rangle$ is depopulated with a rate $(\Gamma_\alpha+\Lambda')$, which in turn, is distributed equally among the states $|\beta\rangle$ and $|\gamma\rangle$, as can be readily seen from the factor of one half multiplying the coefficient of $\rho_{\alpha\alpha}$ in Eqs. (16b) and (16c). The state $|\alpha\rangle$ is also being populated with a rate $1/2\Lambda'$ by the states $|\beta\rangle$ and $|\gamma\rangle$. The state $|\beta\rangle$ ($|\gamma\rangle$) is depopulated at a rate $(\Gamma_\beta+(1/2)\Lambda)$ and repopulated with the same rate from $|\gamma\rangle$ ($|\beta\rangle$). The set (16a)–(16c) can be solved exactly by calculating its eigenvalues and eigenstates, subject to the condition $\rho_{\alpha\alpha}+\rho_{\beta\beta}+\rho_{\gamma\gamma}=1$. This yields the temporal solution

$$\rho_{\alpha\alpha}(t)=\rho_{\alpha\alpha}^{st}+[\rho_{\alpha\alpha}(0)-\rho_{\alpha\alpha}^{st}]e^{-[\Gamma_\alpha+(3/2)\Lambda']t}, \quad (17a)$$

$$\rho_{\beta\beta}(t)=\rho_{\beta\beta}^{st}+\left\{\rho_{\beta\beta}(0)-\rho_{\beta\beta}^{st}+\frac{1}{2}[\rho_{\alpha\alpha}(0)-\rho_{\alpha\alpha}^{st}]\right\}\times e^{-[2\Gamma_\beta+\Lambda-(1/2)\Lambda']t}-\frac{1}{2}[\rho_{\alpha\alpha}(0)-\rho_{\alpha\alpha}^{st}]\times e^{-[\Gamma_\alpha+(3/2)\Lambda']t}, \quad (17b)$$

$$\rho_{\gamma\gamma}(t)=\rho_{\gamma\gamma}^{st}-\left\{\rho_{\beta\beta}(0)-\rho_{\beta\beta}^{st}+\frac{1}{2}[\rho_{\alpha\alpha}(0)-\rho_{\alpha\alpha}^{st}]\right\}\times e^{-[2\Gamma_\beta+\Lambda-(1/2)\Lambda']t}-\frac{1}{2}[\rho_{\alpha\alpha}(0)-\rho_{\alpha\alpha}^{st}]\times e^{-[\Gamma_\alpha+(3/2)\Lambda']t}, \quad (17c)$$

where $\rho_{ii}(0)$ are the initial populations. The steady-state populations, ρ_{ii}^{st} are given by

$$\rho_{\alpha\alpha}^{st}=\frac{\Lambda'}{2\Gamma_\alpha+3\Lambda'}, \quad (18a)$$

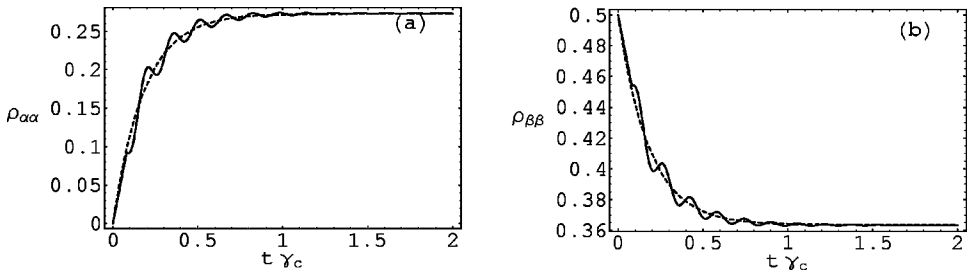

FIG. 3. Time evolution numerical simulation, of dressed-state population $\rho_{\alpha\alpha}$ and $\rho_{\beta\beta}$ obtained by solving Eqs. (13a)–(13f) (solid line), and the approximate solution based on Eqs. (17a)–(17c) (dashed line). The chosen parameters are: $\Omega=20\gamma_c$, $\gamma_b=2\gamma_c$, $G=0.1\gamma_c$, $\Lambda=3\gamma_c$. The time is scaled by γ_c.

$$\rho^{st}_{\beta\beta}=\rho^{st}_{\gamma\gamma}=\frac{\Gamma_\alpha+\Lambda'}{2\Gamma_\alpha+3\Lambda'}. \tag{18b}$$

We can see that the population $\rho_{\beta\beta}$, $\rho_{\gamma\gamma}$ have similar behavior, though not identical, a fact that is not surprising at all in light of the very similar composition of the states $|\beta\rangle$ and $|\gamma\rangle$. The population of the state $|\alpha\rangle$ is unique in the sense that it decays with only one decay constant, while the other populations have a composite decay. Figure 3 shows a comparison between the exact solution for $\rho_{\alpha\alpha}$ and $\rho_{\beta\beta}$ (solid line), obtained by solving numerically the equation set (13a)–(13f), with our approximate analytic solution (17a)–(17c) shown in dashed line. The normalized parameters for the numerical simulation were set to be $\Omega=20\gamma_c$, $\gamma_b=2\gamma_c$, $G=0.1\gamma_c$, $\Lambda=3\gamma_c$. We can see that the population $\rho_{\alpha\alpha}$ is a monotonically increasing, oscillating function of time that reaches a steady-state value $\rho^{st}_{\alpha\alpha}\approx 0.27$. The behavior of $\rho_{\beta\beta}$ is opposite, i.e., it is a monotonically decreasing oscillating function and it reaches the steady-state value $\rho^{st}_{\beta\beta}\approx 0.36$. $\rho_{\gamma\gamma}$ is not shown because of its similarity to $\rho_{\beta\beta}$, due the choice of parameters made. The approximate solutions describe nicely the envelope of oscillation and the correct expression for the steady state. One can see that $\rho^{st}_{\alpha\alpha}<\rho^{st}_{\beta\beta}=\rho^{st}_{\gamma\gamma}$, for any finite Λ, and hence, population inversion do exist in the dressed-state basis. For the transitions $|\alpha\rangle\rightarrow|\beta\rangle$ and $|\alpha\rangle\rightarrow|\gamma\rangle$, the population difference is negative, namely noninversion. For the transitions $|\beta\rangle\rightarrow|\gamma\rangle$ and $|\gamma\rangle\rightarrow|\beta\rangle$, the population difference is zero. It remains to be seen whether these transitions amplify, and thus, result in amplification without inversion in the dressed-state basis. In the strong coupling field limit, $\Omega\gg G$ the steady-state populations become

$$\rho^{st}_{\beta\beta}=\rho^{st}_{\gamma\gamma}=\frac{\gamma_c+\Lambda}{2\gamma_c+3\Lambda}, \tag{19}$$

and

$$\rho^{st}_{\alpha\alpha}=\frac{\Lambda}{2\gamma_c+3\Lambda}. \tag{20}$$

In the following, we will get into more detail regarding gain without inversion in the dressed-state basis.

B. Evolution of coherences

Ignoring the ''nonsecular'' couplings between coherences and populations in Eqs. (13a)–(13f) results in equations that are simpler than the original ones, however, they are still very complicated, particularly the equations for $\rho_{\beta\gamma}$ and its conjugate, which are coupled to all the other coherences. Hence, one would like to further approximate these equations in such a way that the resulting solutions will be fairly simple on one hand, and be a reasonable approximation to the exact solution on the other. We solved numerically the complete set (13a)–(13f) and found that $\rho_{\beta\gamma}$, and hence, its conjugate are substantially larger than the other coherences, indicating the crucial role these coherences play. In light of the above, we couple each atomic coherence to itself (describing the free evolution) and to $\rho_{\beta\gamma}$ and $\rho_{\gamma\beta}$ acting as the dominant source terms.

This gives the following equations:

$$\dot{\rho}_{\alpha\beta}=-(\Gamma_{\alpha\beta}-iR)\rho_{\alpha\beta}-\tilde{\Gamma}'\rho_{\beta\gamma}+(\tilde{\Gamma}-\tilde{\Gamma}')\rho_{\gamma\beta}, \tag{21a}$$

$$\dot{\rho}_{\alpha\gamma}=-(\Gamma_{\alpha\gamma}+iR)\rho_{\alpha\gamma}+(\tilde{\Gamma}-\tilde{\Gamma}')\rho_{\beta\gamma}-\tilde{\Gamma}'\rho_{\gamma\beta}, \tag{21b}$$

$$\dot{\rho}_{\beta\gamma}=-(\Gamma_{\beta\gamma}+2iR)\rho_{\beta\gamma}-\left(\Gamma_\beta+\frac{1}{2}\Lambda-\frac{1}{2}\Lambda'\right)\rho_{\gamma\beta}, \tag{21c}$$

along with the equation for $\rho_{\gamma\beta}=\rho^*_{\beta\gamma}$. Solving the eigenvalue problem of Eqs. (21a)–(21c), we find the transient solutions for the coherences, in the strong coupling field limit. These solutions are

$$\begin{aligned}\rho_{\alpha\beta}(t)=&A\exp[-(\Gamma_{\alpha\beta}-iR)t]\\&+C\frac{(\tilde{\Gamma}-\tilde{\Gamma}')(\Gamma_\beta+\Lambda/2-\Lambda'/2)+i4\tilde{\Gamma}'R}{(\Gamma_\beta+\Lambda/2-\Lambda'/2)(\Gamma_{\beta\gamma}-\Gamma_{\alpha\beta}+3iR)}\\&\times\exp[-(\Gamma_{\beta\gamma}+2iR)t]\\&+D\frac{(\tilde{\Gamma}'-\tilde{\Gamma})+i\tilde{\Gamma}'(\Gamma_\beta+\Lambda/2-\Lambda'/2)/4R}{\Gamma_{\beta\gamma}-\Gamma_{\alpha\beta}-iR}\\&\times\exp[-(\Gamma_{\beta\gamma}-2iR)t],\end{aligned} \tag{22a}$$

$$\rho_{\alpha\gamma}(t)=B\exp[-(\Gamma_{\alpha\beta}+iR)t]$$
$$+C\frac{\tilde{\Gamma}'(\Gamma_\beta+\Lambda/2-\Lambda'/2)-i4R(\tilde{\Gamma}-\tilde{\Gamma}')}{(\Gamma_\beta+\Lambda/2-\Lambda'/2)(\Gamma_{\beta\gamma}-\Gamma_{\alpha\beta}+iR)}$$
$$\times\exp[-(\Gamma_{\beta\gamma}+2iR)t]$$
$$+D\frac{\tilde{\Gamma}'-i(\tilde{\Gamma}-\tilde{\Gamma}')(\Gamma_\beta+\Lambda/2-\Lambda'/2)/4R}{\Gamma_{\beta\gamma}-\Gamma_{\alpha\beta}-3iR}$$
$$\times\exp[-(\Gamma_{\beta\gamma}-2iR)t], \tag{22b}$$

$$\rho_{\beta\gamma}(t)=C\frac{4iR}{\Gamma_\beta+\Lambda/2-\Lambda'/2}\exp[-(\Gamma_{\beta\gamma}+2iR)t]$$
$$+D\,i\frac{\Gamma_\beta+\Lambda/2-\Lambda'/2}{4R}\exp[-(\Gamma_{\beta\gamma}-2iR)t], \tag{22c}$$

where A, B, C, and D are constants ought to be calculated from initial conditions.

The main deficiency of Eqs. (22a)–(22c) is the zero steady-state predicted by them. The reason for this is the omission of the populations source terms in writing Eqs. (21a)–(21c). We have solved analytically Eqs. (21a)–(21c) with the population source terms included. The time-dependent analytical solution obtained was checked against numerical calculations and found to be in excellent agreement. Unfortunately, the solution is so complicated, that even reduction operations carried out by MATHEMATICA [30] could not give a manageable solution. For the purpose of finding the steady-state coherences, it is sufficient to retain the population terms in Eqs. (21a)–(21c), set to zero the time derivatives, and solve the resulting algebraic equations. This yields, using expressions (18a) and (18b) for the steady-state populations, the following steady state coherences:

$$\rho^{st}_{\alpha\beta}=(\rho^{st}_{\alpha\gamma})^*=\frac{(\Gamma_{\alpha\beta}+iR)[\Gamma_\alpha\tilde{\Gamma}'+(\Gamma_\alpha+2\Lambda')(\tilde{\Gamma}+\tilde{\Gamma}')]}{(\Gamma^2_{\alpha\beta}+R^2)(2\Gamma_\alpha+3\Lambda')}$$
$$+\frac{4\Gamma_\beta(\Gamma_{\alpha\beta}+iR)(\Gamma_\alpha+\Lambda')[(2\tilde{\Gamma}'-\tilde{\Gamma})(2\Gamma_\beta+\Lambda-\Lambda'/2)-2iR\tilde{\Gamma}]}{(\Gamma^2_{\alpha\beta}+R^2)(2\Gamma_\alpha+3\Lambda')[\Gamma^2_{\beta\gamma}+4R^2-(\Gamma_\beta+\Lambda/2-\Lambda'/2)^2]}, \tag{23a}$$

$$\rho^{st}_{\beta\gamma}=\frac{4\Gamma_\beta(\Gamma_\alpha+\Lambda')}{2\Gamma_\alpha+3\Lambda'}\frac{(2\Gamma_\beta+\Lambda-\Lambda'/2)-2iR}{(\Gamma_\beta+\Lambda/2-\Lambda'/2)^2-(\Gamma^2_{\beta\gamma}+4R^2)}. \tag{23b}$$

The steady-state values predicted by the last expressions were checked against numerical calculation and found to be in a very good agreement. Note that expressions (23a) and (23b) also give the steady-state dispersion and not only the gain or absorption coefficients. The expected dominance of $\rho_{\beta\gamma}$ on the other two coherences, can be seen by noting that the term $\tilde{\Gamma}+\tilde{\Gamma}'$, appearing in $\rho_{\alpha\beta}$ and $\rho_{\alpha\gamma}$ (but not in $\rho_{\beta\gamma}$) varies like $o(G/R)$, thus, the coherence $\rho_{\alpha\beta}$ varies like $\rho_{\alpha\beta}\sim G/R^2$ while $\rho_{\beta\gamma}$ varies like $\rho_{\beta\gamma}\sim 1/R$. The second term in $\mathrm{Im}(\rho_{\alpha\beta})$ is of the order G/R^3 and can be neglected. Figure 4 shows the exact coherences obtained by solving numerically Eqs. (13a)–(13f) (solid line), and the corresponding approximate analytic solutions formed by $\rho_{ij}(t)+\rho^{st}_{ij}$, as given by expressions (22a)–(22c) and (23a) and (23b). The chosen parameters are the same as in Fig. 3. It can be seen that the approximate analytic solution deviates from the exact one, a deviation that decreases as time goes by. The source for this behavior is the omission of the population source terms in Eqs. (21a)–(21c). However, the oscillation frequency is predicted correctly by the approximate solutions. Moreover, the approximate solution for $\rho_{\beta\gamma}$ appears to be more accurate than the other two, again indicating the crucial role played by $\rho_{\beta\gamma}$ and $\rho_{\gamma\beta}$. Note also the negligible contribution of $\rho_{\alpha\beta}$ and $\rho_{\alpha\gamma}$ to $\rho_{\beta\gamma}$. The latter coherence is not coupled to $\rho_{\alpha\beta},\rho_{\alpha\gamma}$ yet the approximation remains satisfactory. Equation (22c) also shows that $\rho_{\beta\gamma}$ has an almost pure sinusoidal form of frequency $2R$. To the contrary, $\rho_{\alpha\beta}$ and $\rho_{\alpha\gamma}$ have a composite oscillation, being a superposition of frequencies. It can be seen from the numerical solution presented in Fig. 4, that the coherences $\rho_{\alpha\beta}$ and $\rho_{\alpha\gamma}$ possess a definite sign, thus, the corresponding transitions between dressed-states, being either amplified or attenuated. More precisely $\mathrm{Im}(\rho_{\alpha\beta})$ is positive in all the range shown, hence, the transition $|\beta\rangle\rightarrow|\alpha\rangle$ is amplified with population inversion in the dressed-state picture at the frequencies ω_L+R and ω_p+R. The transition $|\alpha\rangle\rightarrow|\gamma\rangle$ is also amplified since $\mathrm{Im}(\rho_{\gamma\alpha})>0$ [Fig. 4(b)], however, without population inversion in this case. This situation is very different from that occurring in the bare-state basis, where the coherences oscillate back and forth across zero, thus experiencing periodic amplification and absorption [12]. In contrast to $\rho_{\alpha\beta}$ and $\rho_{\alpha\gamma}$, the sign of $\mathrm{Im}(\rho_{\gamma\beta})$ is alternating thus the transition $|\beta\rangle\rightarrow|\gamma\rangle$ is being amplified and absorbed periodically. Another feature seen in Fig. 4 is the strength of the coherence $\rho_{\beta\gamma}$, which is seen to be three orders of magnitude stronger than the other two coherences. The transition $|\gamma\rangle\rightarrow|\alpha\rangle$, however is absorbing *despite* the population inversion [see Fig. 4(b)].

Steady-state amplification of the $|\beta\rangle\rightarrow|\alpha\rangle$ transition at frequencies ω_L+R and ω_p+R, occurs whenever $\mathrm{Im}(\rho_{\alpha\beta})$

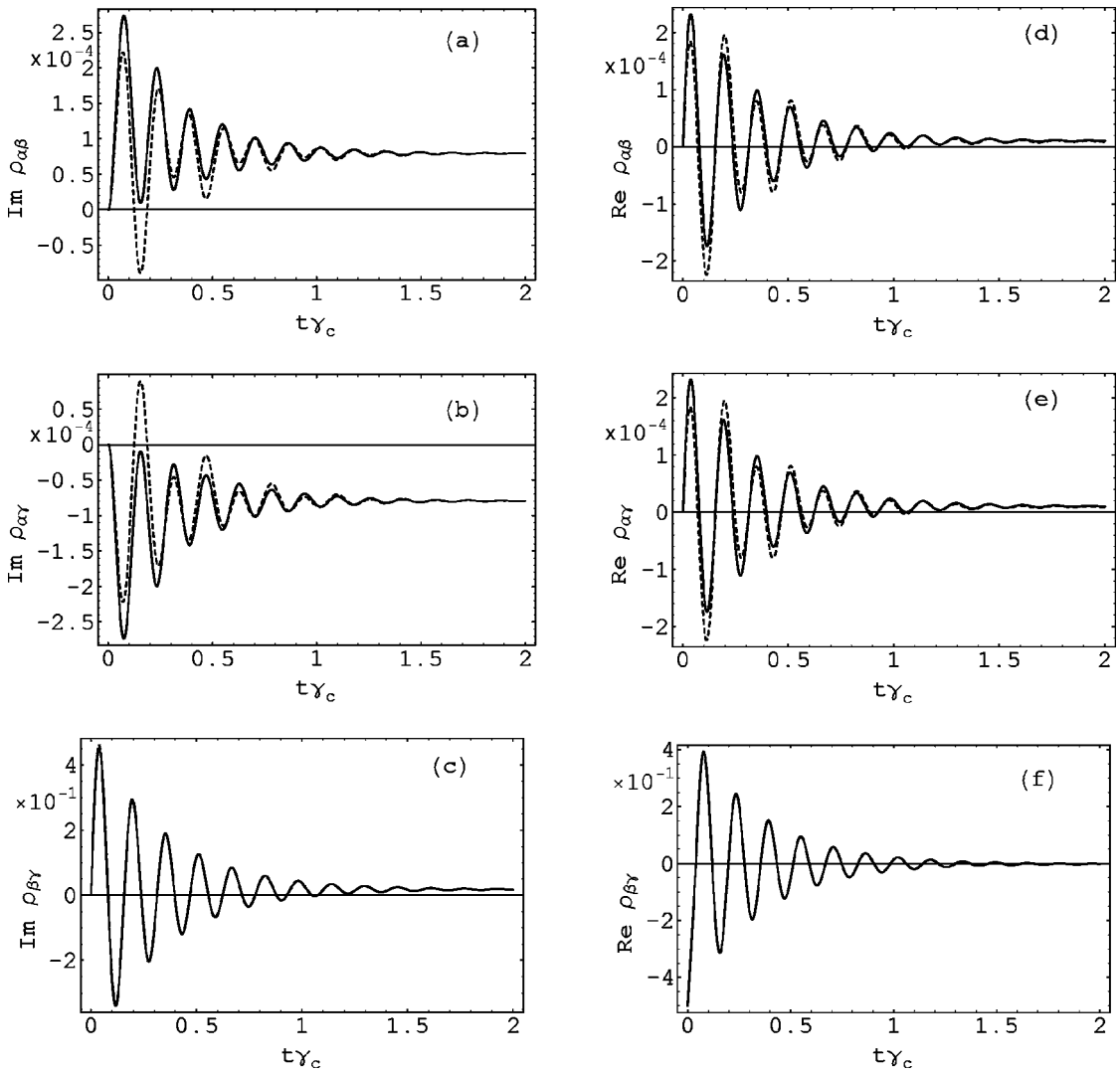

FIG. 4. Normalized time evolution numerical simulation, of dressed-state coherences obtained by solving Eqs. (13a)–(13f) (solid line), and the approximate solution based on Eqs. (22a)–(22c) and (23a) and (23b) (dashed line). The chosen parameters are the same as in Fig. 3. Note the absorption despite population inversion seen in (b).

>0. Taking into account only the first term in Eq. (23a), we find gain in the following two cases.

(1) For any incoherent pump rate Λ (even zero), if $\gamma_b > \gamma_c$. The physical interpretation of this result is clear: if level $|b\rangle$ is drained more quickly than $|c\rangle$ there is no need for the incoherent pump. The disparity between the decay rates γ_b and γ_c acts as an effective incoherent pump. The recycling of the population is accomplished by the coherent probe field, albeit losses.

(2) For $[\Omega^2/\Omega^2+R^2]\gamma_c<\gamma_b<\gamma_c$ provided that the incoherent pump rate is strong enough such that $\Lambda>[\Gamma_\alpha(\gamma_c-\gamma_b)/\Gamma_\alpha-2\Omega^2(\gamma_c-\gamma_b)/R^2]$.

This gain is ''regular'' gain, due to population inversion since $\rho_{\beta\beta}>\rho_{\alpha\alpha}$.

The transition $|\alpha\rangle\rightarrow|\gamma\rangle$ at frequencies ω_L+R and ω_p+R will be amplified for the same range of parameters as stated in items 1 and 2 above because the corresponding gain coefficient is proportional to $\mathrm{Im}(\rho^{st}_{\gamma\alpha})=-\mathrm{Im}(\rho^{st}_{\alpha\gamma})=\mathrm{Im}(\rho^{st}_{\alpha\beta})$. However, this transition is inversionless, and it is due to external field induced quantum interferences and atomic coherences.

In order to interpret the result that gain exists for the case of $\Lambda=0$, we have studied parametricaly the changes that occur in the population of the state $|\alpha\rangle$ and in the coherences. From the numerical solution of the dressed-state system, it can be seen that even when the incoherent pump is zero but $\gamma_b>\gamma_c$, the population of the state $|\alpha\rangle$ is not zero though very small. However, one expects no population in the state $|\alpha\rangle$ when $\Lambda=0$. The mismatch between the decaying rates γ_b and γ_c is the reason for nonzero population in $|\alpha\rangle$ (see Fig. 5). This acts as an effective incoherent pump. Indeed, when $\Lambda=0$ and $\gamma_b=\gamma_c$, no incoherent pump, effective or direct, is present and it is found that $\rho_{\alpha\alpha}$ vanishes, as it should.

Studying the coherences by applying the full numerical calculation, one finds gain even if no incoherent pump is present. Figure 6 displays such a gain for inversionless tran-

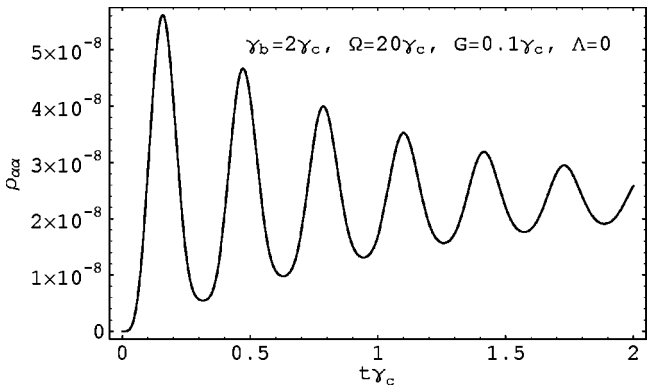

FIG. 5. Population of state α, $\rho_{\alpha\alpha}$ for zero incoherent pump rate and nonequal decaying rates. The chosen parameters are the same as in Fig. 3.

sition $|\alpha\rangle \rightarrow |\gamma\rangle$ for the case $\Lambda=0$ and nonequal decay rates, i.e., $\gamma_b > \gamma_c$. Figure 7 exhibits gain for the same transition but for nonzero incoherent pump rate and equal decaying rates. Only when the decaying rates are equal and the incoherent pump rate is zero, we effectively turn off the interference effect by causing $\tilde{\Gamma}=0, \tilde{\Gamma}'=0$ and both the imaginary and the real parts of the coherences $\rho_{\alpha\beta}$ and $\rho_{\alpha\gamma}$ vanish. As a consequence, the gain vanishes. Again this indicates that the mismatch in the decay rates acts effectively as incoherent pump.

Gain in the dressed-state picture occurs strictly at the dressed frequencies, $\omega_i \pm \mathrm{R}$ $(i=L,p)$, which are shifted from those of the bare state basis. However, no such frequencies exist in the bare-state representation. We believe that the appropriate basis to use is the dressed basis, when dealing with strong fields.

The opposite transition, $|\gamma\rangle \rightarrow |\alpha\rangle$ at frequencies $\omega_L - R$ and $\omega_p - R$, exhibits absorption with population inversion [see Fig. 4(b)]. In a sense, this is the reverse process of amplification without inversion and it is explained as a constructive quantum interference for the stimulated absorption process. The $|\beta\rangle \rightarrow |\gamma\rangle$ transition, at frequencies $\omega_L + 2R$ and $\omega_p + 2R$ will be absorbed, since the term $4R^2$ appearing in the denominator of Eq. (23b) far exceeds the other denominator terms, resulting in $\mathrm{Im}(\rho_{\gamma\beta}) < 0$, and hence absorption.

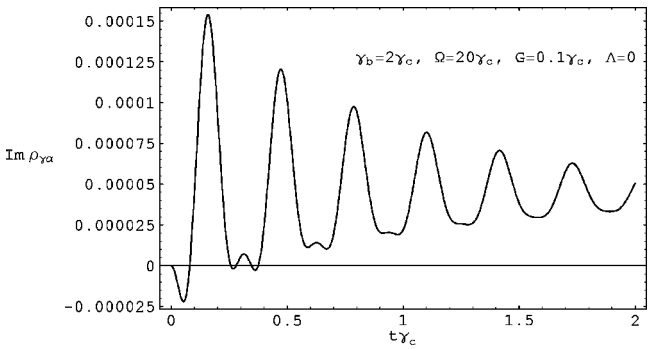

FIG. 6. $\mathrm{Im}(\rho_{\gamma\alpha})$ as a function of normalized time parameter $\gamma_c t$ for the case of zero incoherent pump rate, $\Lambda=0$, exhibiting gain for the $|\alpha\rangle \rightarrow |\gamma\rangle$ transition for most of the region and especially at steady state. The chosen parameters are the same as in Fig. 3.

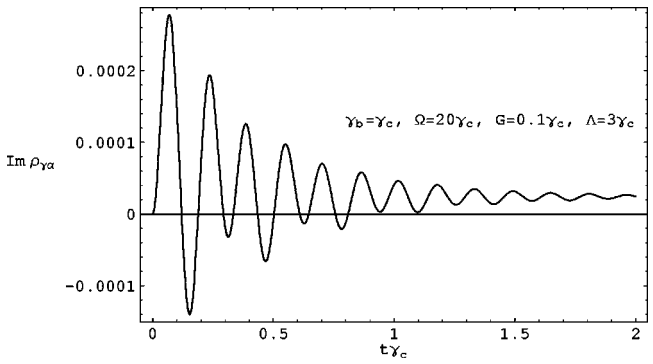

FIG. 7. $\mathrm{Im}(\rho_{\gamma\alpha})$ as a function of normalized dimensionless time parameter $\gamma_c t$ for the case of nonzero incoherent pump rate, and equal decaying rates $\gamma_b = \gamma_c$. The transition possess gain the steady-state regime. The chosen parameters are the same as in Fig. 3.

The transition $|\gamma\rangle \rightarrow |\beta\rangle$ in turn, at frequencies $\omega_L - 2R$, $\omega_p - 2R$ will be amplified for any incoherent pump rate.

Utilizing the strong driving field limit, once again, the imaginary parts of the steady-state coherences can be expressed in terms of the original atomic parameters as

$$\mathrm{Im}(\rho^{st}_{\alpha\beta}) = \mathrm{Im}(\rho^{st}_{\gamma\alpha}) = G\frac{(\gamma_c + 2\Lambda)(\gamma_b - \gamma_c) + \gamma_c\Lambda}{2\sqrt{2}\Omega^2(2\gamma_c + 3\Lambda)}, \tag{24a}$$

$$\mathrm{Im}(\rho^{st}_{\beta\gamma}) = \frac{\gamma_b(\gamma_c + \Lambda)}{2\Omega(2\gamma_c + 3\Lambda)}. \tag{24b}$$

As mentioned before, in the strong coupling field limit (weak probe) the state $|\alpha\rangle$ degenerates into the highest excited bare state $|c\rangle$, thus, we are facing a situation of full *noninversion* in the dressed-state basis, i.e., $\rho_{cc} < \rho_{\beta\beta} = \rho_{\gamma\gamma}$ [see Eqs. (19)–(20)]. Equation (24a) indicates that gain can be obtained for the $|c\rangle \rightarrow |\beta\rangle$ and $|c\rangle \rightarrow |\gamma\rangle$ transitions (the Autler-Townes transitions [31]) for the following conditions.

(1) For any incoherent pump rate Λ if $\gamma_b > \gamma_c$.

(2) For $1/2\gamma_c < \gamma_b < \gamma_c$, provided that $\Lambda > [\gamma_c(\gamma_c - \gamma_b)/2\gamma_b - \gamma_c]$.

This gain is *without inversion*. The physics involved in this condition is as follows: It states that the dephasing time of level $|c\rangle$ namely $(1/2\gamma_c)^{-1}$ must be longer than any other decay time in the system. The dephasing process must be slow with respect to other processes in order to preserve the phase of the dipole transition ρ_{ac}. This makes possible the quantum coherent effect whereby the interference can result in gain without inversion.

To improve the temporal results for the populations we retained only the dominant coherences, namely, $\rho_{\beta\gamma}$ and $\rho_{\gamma\beta}$ in the population equations [Eqs. (16a)–(16c)] serving as source terms. That is, we seek the particular solution to the set

$$\dot{\rho}_{\alpha\alpha}=-(\Gamma_\alpha+\Lambda')\rho_{\alpha\alpha}+\frac{1}{2}\Lambda'\rho_{\beta\beta}+\frac{1}{2}\Lambda'\rho_{\gamma\gamma}-\frac{1}{2}\Lambda'(\rho_{\beta\gamma}+\rho_{\rho_{\gamma\beta}}), \tag{25a}$$

$$\dot{\rho}_{\beta\beta}=-\left(\Gamma_\beta+\frac{1}{2}\Lambda\right)\rho_{\beta\beta}+\frac{1}{2}(\Gamma_\alpha+\Lambda')\rho_{\alpha\alpha}+\left(\Gamma_\beta+\frac{1}{2}\Lambda-\frac{1}{2}\Lambda'\right)\rho_{\gamma\gamma}+\frac{1}{4}\Lambda'(\rho_{\beta\gamma}+\rho_{\rho_{\gamma\beta}}), \tag{25b}$$

$$\dot{\rho}_{\gamma\gamma}=-\left(\Gamma_\beta+\frac{1}{2}\Lambda\right)\rho_{\gamma\gamma}+\frac{1}{2}(\Gamma_\alpha+\Lambda')\rho_{\alpha\alpha}+\left(\Gamma_\beta+\frac{1}{2}\Lambda-\frac{1}{2}\Lambda'\right)\rho_{\beta\beta}+\frac{1}{4}\Lambda'(\rho_{\beta\gamma}+\rho_{\rho_{\gamma\beta}}), \tag{25c}$$

where we take for $\rho_{\beta\gamma}$ and $\rho_{\gamma\beta}$ only the leading terms in Eq. (22c). These equations are integrated giving the following results:

$$\rho_{\alpha\alpha}(t)=\rho_{\alpha\alpha}^{st}+c_1e^{-[\Gamma_\alpha+(3/2)\Lambda']t}+\rho_{\alpha\alpha}^{par}(t), \tag{26a}$$

$$\rho_{\beta\beta}(t)=\rho_{\beta\beta}^{st}-\frac{1}{2}c_1e^{-[\Gamma_\alpha+(3/2)\Lambda']t}+c_2e^{-[2\Gamma_\beta+\Lambda-(1/2)\Lambda']t}-\frac{1}{2}\rho_{\alpha\alpha}^{par}(t), \tag{26b}$$

$$\rho_{\gamma\gamma}(t)=\rho_{\gamma\gamma}^{st}-\frac{1}{2}c_1e^{-[\Gamma_\alpha+(3/2)\Lambda']t}-c_2e^{-[2\Gamma_\beta+\Lambda-(1/2)\Lambda']t}-\frac{1}{2}\rho_{\alpha\alpha}^{par}(t), \tag{26c}$$

where the particular solution is given by

$$\rho_{\alpha\alpha}^{par}(t)=-\frac{\rho_{\beta\gamma}(0)\Lambda'[(\Gamma_\alpha+\frac{3}{2}\Lambda'-\Gamma_{\beta\gamma})\cos(2Rt)+2R\sin(2Rt)]}{(\Gamma_\alpha+\frac{3}{2}\Lambda'-\Gamma_{\beta\gamma})^2+4R^2}\quad e^{-\Gamma_{\beta\gamma}t}.$$

The integration constants are given in terms of initial populations and coherences by

$$c_1=\rho_{\alpha\alpha}(0)-\rho_{\alpha\alpha}^{st}-\rho_{\alpha\alpha}^{par}(0)$$

$$c_2=\rho_{\beta\beta}(0)-\rho_{\beta\beta}^{st}+\frac{1}{2}[\rho_{\alpha\alpha}(0)-\rho_{\alpha\alpha}^{st}].$$

Figure 8 shows the difference between the exact population $\rho_{\alpha\alpha}$ and the approximate solution (26a)–(26c). It can be seen that the approximate solution is very accurate.

To compare with the steady-state situation in the bare-state basis, we need to transform back to the bare-state basis, via the the matrix product $\rho^B=T^{-1}\rho^{Dr}T$, where ρ^{Dr} is the density matrix in the dressed-state basis, formed by the steady-state populations and coherences of Eqs. (18a)–(18b) and (23a) and (23b). Further utilization of the strong coupling field limit gives bare-state populations, in the steady-state regime.

$$\rho_{aa}=\rho_{bb}=\frac{\gamma_c+\Lambda}{2\gamma_c+3\Lambda}, \tag{27a}$$

and

$$\rho_{cc}=\frac{\Lambda}{2\gamma_c+3\Lambda}. \tag{27b}$$

The bare state coherences are

$$\rho_{ab}=-i\frac{\gamma_b(\gamma_c+\Lambda)}{2\Omega(2\gamma_c+3\Lambda)}, \tag{28a}$$

$$\rho_{ac}=iG\frac{\Lambda(\gamma_b-\gamma_c)-\gamma_c^2}{2\Omega^2(2\gamma_c+3\Lambda)}, \tag{28b}$$

and

$$\rho_{bc}=\frac{G\gamma_c}{\Omega(2\gamma_c+3\Lambda)}. \tag{28c}$$

In obtaining the expressions for populations and coherences, we find that our general form reduce to previously obtained results [12].

We see that in the bare-state basis one always has $\mathrm{Im}(\rho_{ab})<0$, thus the coupling laser is always attenuated. The probe transition exhibits inversionless gain for $\gamma_b>\gamma_c$ for pump rates satisfying $\Lambda>\gamma_c^2/\gamma_b-\gamma_c$. From the analysis presented above, we conclude that for a weak probe, true lasing without population inversion can be realized, both in the bare-state and the dressed-state basis.

V. SPECTRAL SHAPE OF THE COHERENCES

The results obtained above for the populations and coherences were derived in the interaction representation. In order to gain knowledge regarding the true frequencies, we must transform back to the Schrödinger representation, though

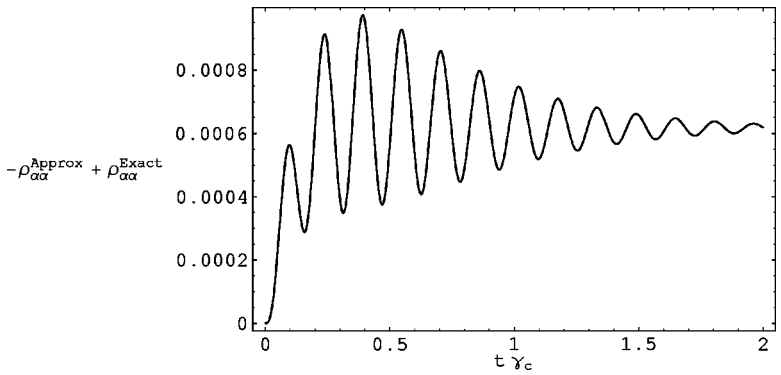

FIG. 8. Difference between exact population $\rho_{\alpha\alpha}$ obtained by solving Eqs. (13a)–(13f) and the approximate solutions based on solutions (26a)–(26c). The chosen parameters are the same as in Fig. 3.

still remaining within the framework of the dressed-state representation.

The Schrödinger picture bare-state density operator ρ_S^B is related to the interaction picture density operator ρ_I^B via the unitary transformation

$$\rho_S^B = U_0 \rho_I^B U_0^\dagger, \tag{29}$$

where $U_0 = e^{-iH_0 t/\hbar}$ is the free evolution matrix. The Schrödinger picture dressed-state density operator is expressed in terms of the bare-state operator via the following rotation:

$$\rho_S^D = T^{-1}\rho_S^B T = (T^{-1}U_0^B T)(T^{-1}\rho_I^B T)[T^{-1}(U_0^B)^\dagger T] = U_0^D \rho_I^D (U_0^D)^\dagger. \tag{30}$$

Here, U_0^D and ρ_I^D are the dressed-state evolution and density operators, respectively. The Schrödinger picture dressed-states coherences show several frequencies. However, the expressions for the density-matrix elements are extremely complex and will not be presented here. The main features are oscillating term at resonance frequencies, ω_p, ω_L and at the Rabi shifted side bands, namely, $\omega_i \pm R$, $\omega_i \pm 2R$ $(i = L, p)$, and other combinations.

These results determine only the existence of gain without inversion or absorption with inversion as well as usual gain with inversion. The relevant polarizations oscillate at the Rabi frequency. However, they do not determine the frequencies at which gain and absorption occur. The procedure to determine that is taking the Fourier transform of the autocorrelation function of these quantities. Due to the extreme complexity of these terms, we have resorted to numerical calculations that aids in determining the frequencies that play role in the gain/absorption processes. These calculations do not provide the spectrum itself, but rather it is the absolute value of the transform of the density-matrix elements, $\rho_{\alpha\beta}$, etc. The numerical results indicate that the polarizations oscillate at ω_L, ω_p, $\omega_p - \omega_L$ and at the Rabi and modulated beat frequencies.

A typical result of these calculations is displayed in Fig. 9 in which we find spectral features at ω_p, $\omega_p - R$, $\omega_p - 2R$. Similar characteristics are also found at and around ω_L and $\omega_p - \omega_L$. Details of these calculations will be shown elsewhere in which a study of the parameter space will be shown.

The experimental studies by Zibrov, Padmabandu, and Kitching and Hollberg [20–22] have shown gain without inversion at resonance, at about ω_p, and absorption at the Rabi sidebands. These results are obtained theoretically in the bare-sate picture by various authors as well as our own bare-state picture calculations, which reproduce the experimental results. However, the dressed-state picture provides insight in the true light matter interaction and in particular, a host of frequencies that could not be obtained in the bare-state picture.

It is more complicated to work and interpret the results in the dressed-state picture, but it reveals many features undetected in the bare-state formalism. The search for the exact parameters that correlates with the experiments is the key, as it is the key in the experiment. This is pursued theoretically. At the present state of the calculations, it is clear in principle that one can obtain the correct gain and absorption spectrum by extensive parameter search.

VI. SUMMARY

Absorption in the presence of inversion and amplification without inversion in a three-level *V*-type system are found in the dressed-state picture. Both of these effects are the manifestation of the quantum interference that occurs in multilevel systems. Moreover, the above two processes constitute a manifestation of a complementarity principle.

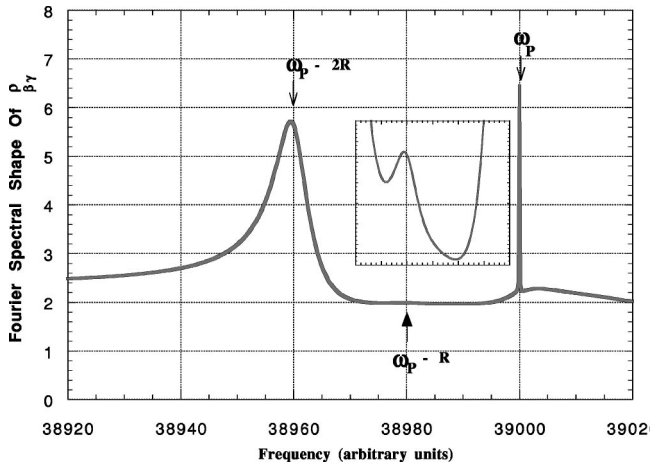

FIG. 9. Spectral line shape of $\rho_{\beta\gamma}$ in the vicinity of ω_p. The system parameters are the same as in Fig. 3. The inset shows a peak at $\omega_p - R$.

We have presented an analysis of light amplification without population inversion in this system within the framework of the dressed-state basis. The equations of motion for the elements of the density matrix are derived from the master equation. In the dressed-state picture, relaxation terms are defined that are related directly to the coherently prepared states and the quantum interference effects. Interference terms are identified. They are shown to be the source for amplification without inversion and for absorption despite the inversion. Consequently, approximate analytical time-dependent solutions for dressed-state populations and coherences were obtained. Comparison of these approximate solutions with the numerically calculated quantities shows excellent agreement. Both of these solutions exhibit the familiar Rabi oscillations. Steady-state density-matrix elements were also calculated, from which we have concluded that for a weak probe field, true lasing without inversion exist for appropriate incoherent pump rate, i.e., lasing without inversion in any state basis. Steady-state quantities were transformed back to the bare-state basis, and were found to be in perfect agreement with results in the literature. Conditions for inversionless gain and ADI were obtained.

Gain is predicted at resonance frequencies and at the Rabi side bands, depending on the relevant parameters. Experimental results have presented gain without inversion at resonance frequency and at frequencies displaced from resonance by about the Rabi frequency in agreement with the present findings. It appears that the dressed-state picture is quite complicated revealing possible amplification without population inversion and absorption with population inversion, two counterintuitive processes prompted by quantum interferences. Thus, interpretation of experimental results becomes extremely subtle. In the present calculation, two fields are included and the dressing is caused by both the pump and probe lasers. Experimentaly, it would be intersting to applay another field, weak enough to avoid further dressing, in order to probe the above-calculated quantum interference processes at resonance, beat, and at the relevant Rabi-shifted frequencies.

Finally, the feature of ADI, absorption despite population inversion, found in this calculation emphasizes the importance of quantum interference. Quantum interference is thus shown to imprint its effect on the processes in the dressed-state picture.

[1] S.E. Harris, Phys. Rev. Lett. **62**, 1033 (1989).
[2] M.O. Scully, S.Y. Zhu, and A. Gavrielides, Phys. Rev. Lett. **62**, 2813 (1989).
[3] G.S. Agrawal, Phys. Rev. A **44**, R28 (1991).
[4] L.M. Narducci *et al.*, Opt. Commun. **81**, 379 (1991).
[5] O. Kocharovskaya, P. Mandel, and Y.V. Radeonychev, Phys. Rev. A **45**, 1997 (1992).
[6] Y. Zhu, Phys. Rev. A **45**, R6149 (1992).
[7] G. Grynberg and C. Cohen-Tannoudji, Opt. Commun. **96**, 150 (1993).
[8] G.A. Wilson, K.K. Meduri, P.B. Sellin, and T.W. Mossberg, Phys. Rev. A **50**, 3394 (1994).
[9] Gautam Vemuri, K.V. Vasavada, and G.S. Agarwal, Phys. Rev. A **52**, 3228 (1995).
[10] Yang Zhao, Danhong Huang, and Cunkai Wu, J. Opt. Soc. Am. B **13**, 1614 (1996).
[11] N.A. Ansari and A.H. Toor, J. Mod. Opt. **43**, 2425 (1996).
[12] Y. Zhu, Phys. Rev. A **53**, 2742 (1996).
[13] G. Grynberg, M. Pinard, and P. Mandel, Phys. Rev. A **54**, 776 (1996).
[14] Gautam Vemuri and G.S. Agarwal, Phys. Rev. A **53**, 1060 (1996).
[15] Shi-Yao Zhu, De-Zhong Wang, and Jin-Yue Gau, Phys. Rev. A **55**, 1339 (1997).
[16] Jacob B. Khurgn and Emmanuel Rosencher, J. Opt. Soc. Am. B **14**, 1249 (1997).
[17] J.L. Cohen and P.R. Berman, Phys. Rev. A **55**, 3900 (1997).
[18] Marlan O. Scully and Shi-Yao Zhu, Phys. Rev. Lett. **62**, 2813 (1989).
[19] A. Imamoglu, J.E. Field, and S.E. Harris, Phys. Rev. Lett. **66**, 1154 (1991).
[20] A.S. Zibrov *et al.*, Phys. Rev. Lett. **75**, 1499 (1995).
[21] G.G. Padmabandu *et al.*, Phys. Rev. Lett. **76**, 2053 (1996).
[22] J. Kitching and L. Hollberg, Phys. Rev. A **59**, 4685 (1999).
[23] Y. Zhu and J. Lin, Phys. Rev. A **59**, 4685 (1999); **53**, 1767 (1996).
[24] Gautam Vemuri, G.S. Agarwal, and B.D. Nageswara, Phys. Rev. A **54**, 3695 (1996).
[25] P.B. Sellin, G.A. Wilson, K.K. Meduri, and T.W. Mössberg, Phys. Rev. A **54**, 2402 (1996).
[26] Y. Zhu, A.I. Rubiera, and Min Xiao, Phys. Rev. A **53**, 1065 (1996).
[27] G.S. Agarwal, Phys. Rev. Lett. **67**, 980 (1991).
[28] M.O. Scully, Phys. Rep. **219**, 191 (1992).
[29] Clude Cohen-Tanudji, Jacques Dupont-Roc, and Gilbert Grynberg, *Atom-Photon Interactions* (Wiley, New York, 1992), p. 428.
[30] MATHEMATICA A System for Doing Mathematics by Computer, Wolfram research (unpublished).
[31] S.H. Autler and C.H. Townes, Phys. Rev. **100**, 703 (1955).